Available online at www.sciencedirect.com
ScienceDirect
Advances in Space Research 38 (2006) 2418–2423
ADVANCES IN SPACE RESEARCH (a COSPAR publication)
www.elsevier.com/locate/asr

Inter-annual variation of gravity waves in the Arctic and Antarctic winter middle atmosphere

Jonathan H. Jiang [a,*], Stephen D. Eckermann [b], Dong L. Wu [a], Ding Yi Wang [c]

[a] Jet Propulsion Laboratory, California Institute of Technology, 4800 Oak Grove Drive, Mail-Stop 183-701, Pasadena, CA 91109, USA
[b] Middle Atmosphere Dynamics Section, Naval Research Laboratory, Washington, DC, USA
[c] Forschungszentrum Karlsruhe GmbH und Universität Karlsruhe, Institut für Meteorologie und Klimaforschung, Karlsruhe, Germany

Received 8 September 2004; received in revised form 7 September 2005; accepted 13 September 2005

Abstract

High latitude, middle atmospheric (28–80 km) gravity wave observations from the Microwave Limb sounder (MLS) on the Upper Atmosphere Research Satellite (UARS) are available during five Arctic and Antarctic winters between 1991 and 1997. Newer data from NOAA Advanced Microwave Sounding Unit (AMSU) instruments have been introduced recently, in order to extend the gravity wave measurements from 1998 to present. Analyses of MLS and AMSU data show substantial inter-annual variability in both magnitude and spatial patterns of gravity wave activity at both Arctic and Antarctic latitudes.

Keywords: Arctic; Antarctic; Middle atmosphere; Gravity wave; UARS MLS; Satellite observation

1. Introduction

It is well known that global scale gravity wave drag provides an important driving force to the stratospheric and mesospheric circulation. Polar winter stratospheric temperatures can be significantly affected by gravity waves through wave-drag driven descent (Austin et al., 2003). Annual warming in the Arctic vortex core's upper stratosphere has been related to the increased gravity wave activity within the Arctic vortex jet-stream (Duck et al., 1998, 2001). Gravity waves can also affect stratospheric temperature directly through the temperature fluctuations these wave motions produce via adiabatic ascent/descent of air parcels. Gravity waves forced by flow over mountains in northern winter high-latitudes have been shown to reach the stratopause level (e.g., Jiang et al., 2004a). In the lower stratosphere, such waves have been found to produce temperature decreases at the ascent phase of the wave that drop local temperatures below critical temperatures for formation of nitric acid trihydrate (NAT) or ice, leading to formation of mountain wave-induced polar stratospheric clouds (PSCs) (e.g., Dörnbrack et al., 2002). These important observations have prompted modelers to consider the overall impact of wintertime high-latitude gravity waves on the polar PSC formation, denitrification and heterogeneous ozone loss (e.g., Carslaw et al., 1999; Dhaniyala et al., 2002; Fueglistaler et al., 2002).

This study summarizes hemispheric patterns and inter-annual variations of wintertime gravity waves in the high-latitude Arctic and Antarctic middle atmosphere observed by UARS MLS. New dataset from NOAA AMSU is also briefly introduced.

2. UARS MLS observations

The atmospheric radiance data collected by UARS MLS during 1991–1997 have been used to extract the global gravity wave variance data since the mid-1990s (Wu and Waters, 1996). Since then, the MLS gravity wave data has been extensively studied and validated to obtain information on global and regional gravity wave climatology

* Corresponding author. Tel.: +1 818 354 7135; fax: +1 818 393 5065.
E-mail address: jonathan@mls.jpl.nasa.gov (J.H. Jiang).

0273-1177/$30
doi:10.1016/j.asr.2005.09.036

and its inter-annual variations (e.g., Wu and Waters, 1997; Jiang et al., 2004b). Combined model-data analysis has associated many of the sources of gravity wave in the MLS data to surface orography (e.g., Jiang et al., 2002, 2004a) and tropospheric convection (McLandress et al., 2000; Jiang et al., 2004b). Cross-comparisons of MLS gravity wave data with gravity wave variances extracted from other ground based and other satellite data have begun to conduct (e.g., Jiang et al., 2002; Wu, 2004).

Recent modeling and data analysis studies (e.g., Jiang et al., 2004a; Wu and Jiang, 2002) have shown that UARS MLS has greatest sensitivity to gravity waves measured at high-latitudes (±45° to ±75°) during both Arctic and Antarctic winters. Fig. 1 shows polar maps of MLS normalized radiance temperature variances (defined as $T_b'^2/T_b^2$, where T_b is the radiance and T_b' is radiance perturbation. See, e.g., Wu and Jiang (2002)) at altitudes 28, 38, 48, 61, and 80 km, averaged using limb scan data acquired during northern winter (December–February 1991–1994; left column), and southern winter (June–August 1992–1994; right column), respectively. These climatological maps show distinct gravity wave patterns (white-color indicates maximum wave activity) throughout the middle atmosphere. While much of this structure is associated with instrumental visibility effects to gravity waves that vary with varying horizontal wind speeds (Alexander, 1998; McLandress et al., 2000; Jiang et al., 2004a), many detailed features can be associated with mountain waves forced by flow over specific mountainous terrain (Jiang et al., 2002, 2004a). These include northern mountain ranges in Europe, North America, Greenland, Iceland, and southern mountain ranges such as Andes, New Zealand and Palmer Peninsula of Antarctic. Above the stratopause, gravity waves are expected to dissipate and a gradual change in geographical pattern with altitude might be expected. Such changes are seen in Fig. 1. For example, the orographic waves over central Eurasia disappear above ~50 km which shift the peak of the remaining wave activities to a region across the northern Atlantic, from Western Europe to Canadian east coast. In the case of southern high latitudes, orographic waves over the Andes and New Zealand seem to persist all the way to 80 km. The relative roles of dissipation and visibility effects in producing these changes are still not completely clear (Alexander, 1998; Jiang et al., 2004a).

Fig. 2 plots the gravity wave momentum fluxes and net wave mean flow accelerations (wave drags) inferred from the normalized MLS radiances using an empirical method described by Jiang and Wang (in preparation). The westward momentum flux is computed using MLS limb-scan radiance variances measured from (1) north-looking descending (ND) orbits and averaged for northern latitudes 45–65°N; (2) south-looking ascending (SA) orbits and averaged for southern latitudes 45–65°S. At these latitudes, the ND and SA measurements are mostly sensitive to gravity waves propagating westward with respect to the mean flow. The eastward momentum fluxes are computed using north-looking ascending (NA) and south-looking descending (SD) measurements for the same northern and southern latitudes, respectively. The NA and SD measurements are mostly sensitive to eastward propagating gravity waves (see Jiang et al., 2003). The magnitude of the MLS-inferred westward momentum fluxes for both north and south latitudes are stronger then those associated with the eastward fluxes. This momentum-flux asymmetry results a net inferred westward wave-induced mean-flow acceleration on the mostly eastward wintertime jets (Fig. 2, right panel), especially at the stratopause level. Duck et al. (2001) have argued that, in presence of strong gravity wave activity in the stratospheric vortexes, the balance among wave drag, pressure gradient, and the Coriolis force could lead to small poleward acceleration to the zonal flow. This could cause a warming in the stratospheric vortex core.

Fig. 2 also shows a vertical growth of gravity wave strength in the stratosphere until the stratopause altitude (~50 km). Above that level, there is an almost zero growth rate for both the south and north waves, possibly due to wave breaking or saturation at the stratopause (Wu, 2001; Duck et al., 2001) and/or to instrumental visibility effects (e.g., Alexander, 1998; Jiang et al., 2004a).

The time evolution of the high-latitude gravity waves is shown in Fig. 3 at 48 and 80 km. Our analyses found that high-latitude stratospheric (28–53 km) gravity waves are strongly seasonal-dependant, peaking in wintertime and weakening in summertime. Thus, the waves MLS resolves in the Arctic vortex region have largest amplitudes during December–February and the waves in the Antarctic vortex have largest amplitudes mostly in June–August, consistent with results from previous studies (e.g., Eckermann et al., 1995). Near the mesopause (~80 km), however, the wave activity has a semiannual variation, peaking in both winter and summer. Semiannual variations in high-latitude mesospheric gravity wave activity have been noted previously in ground-based radar wind data (e.g., Manson et al., 1997). Since both wind speeds and gravity wave variances have been observed to vary semiannually at mesospheric heights (e.g., Vincent and Fritts, 1987), the role of semiannual variations in the mesospheric wind speeds in modulating the MLS visibility to gravity waves must also be borne in mind here, when interpreting observed variations in MLS variances.

Analyses of MLS observed high-latitude gravity waves also reveal substantial inter-annual variations in both wave magnitude and its geographical distribution. For example, there is an increasing trend of wave variances during late February from 1992 to 1994 as indicated by the small black-arrows in Fig. 3. Also, gravity wave variances in late June decrease from 1992 to 1994 as shown by the small red-arrows. Other notable variations are: December to early-January 1992–1993 shows the strongest wave magnitude comparing to the same period in 1991–1992 and in 1993–1994; Late-August of 1994 has the weakest wave magnitude comparing to late-August in 1993 and in 1992. To see what could cause the above inter-annual variations, Fig. 4 plots hemispheric maps of stratospheric gravity wave

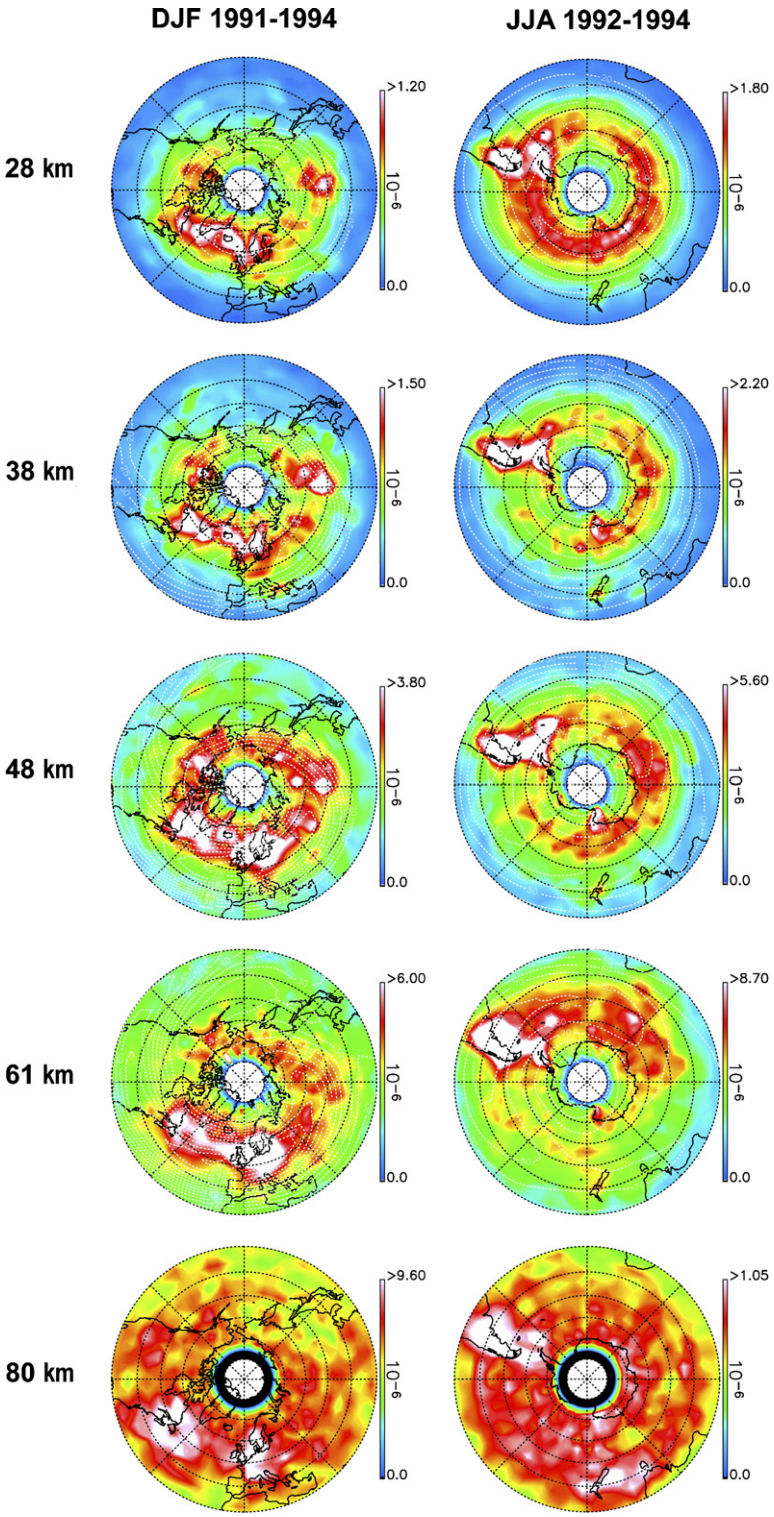

Fig. 1. Polar orthographic maps of wintertime normalized radiance temperature variance at 28, 38, 48, 61 and 80 km altitudes, computed using MLS limb-scan north-looking measurements for northern winter (left column) and south-looking data for southern winter (right column). These fields are averaged over period of December–February 1991–1994 for north winter and June–August 1992–1994 for south winter, respectively. The dotted white contours are the United Kingdom Meteorological Office (UKMO) reanalysis winds at about same altitudes and averaged over the MLS measurement days that went into this variance map. No UKMO wind data available at 80 km.

variance at an altitude 38 km during winter months of each MLS measurement year for: (1) Arctic region 15–31 December mean (first row), (2) Arctic region 15–28 February mean (second row), (3) Antarctic region 15–30 June mean (third row) and (4) Antarctic region 15–31 August mean (forth row). The maps in the left three columns of

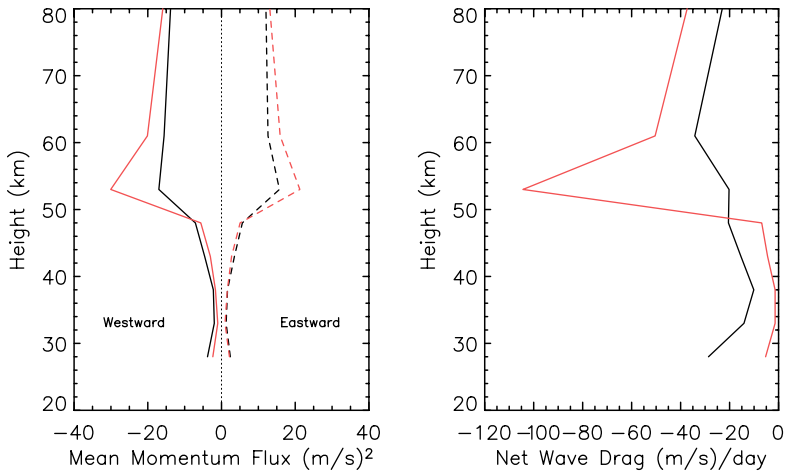

Fig. 2. The profiles in the left panel are the momentum fluxes densities per unit mass ($m^2 s^{-2}$) associated with the gravity waves longitudinal averaged (1) for December–February 1991–1994 between 45°N and 65°N (black), and (2) for June–August 1992–1994 between 45°S and 65°S (red). The solid-lines are for the westward-propagating waves measured from MLS ND or SA orbits; the dashed-lines are for the eastward-propagating waves measured from NA or SD orbits. The right panel shows the net wave-induced mean flow acceleration ($m s^{-1} day^{-1}$) computed from the difference between the westward and the eastward momentum fluxes. The negative values of wave drag indicate a westward drag force.

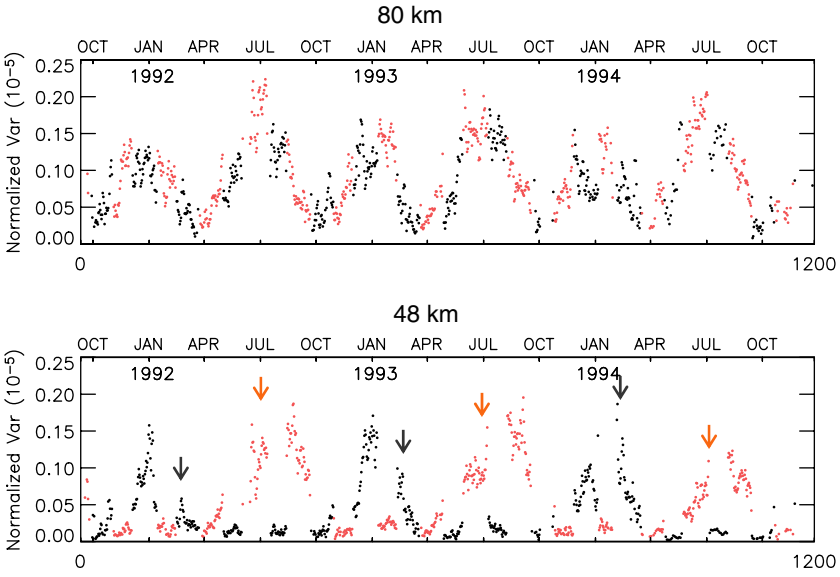

Fig. 3. Time-series of daily-mean MLS limb-scan normalized radiance variances for the normal-scan period (October 1991–November 1994) at 48 km (lower panel) and 80 km (top panel). The black-dots represent the gravity wave variances at high northern latitudes as measured from UARS MLS north-looking orbits and averaged between 45°N and 75°N; the red-dots show the southern high latitude gravity wave variances averaged for 45–75°S. A 3-day running mean was applied to the daily averages to smooth-out the large fluctuations in the daily variances.

Fig. 4 are computed using MLS data measured during the normal-scan period (October 1991–November 1994), which is mostly continuously available for each of the full half-month periods. The maps in the right two columns are computed using MLS data obtained during the reverse-scan period, in which the data are more intermittent and sparse.

First, we see substantial variations in mean vortex winds (over-plotted in white) from year to year, particularly in the north, highlighting the well-known strong inter-annual variability of the Arctic winter stratosphere due to Rossby wave driving (e.g., Waugh and Rong, 2002). Gravity wave variances from year-to-year in Fig. 4 correlate reasonably well with variations in peak vortex winds, consistent with visibility effects since gravity waves become more visible to MLS when winds are strong and less visible when they are weak (e.g., Jiang et al., 2004a). Nonetheless, strong zonal asymmetries are consistent with source effects, such as strong peaks over southern South America and the Palmer Peninsula consistent with mountain waves (Jiang

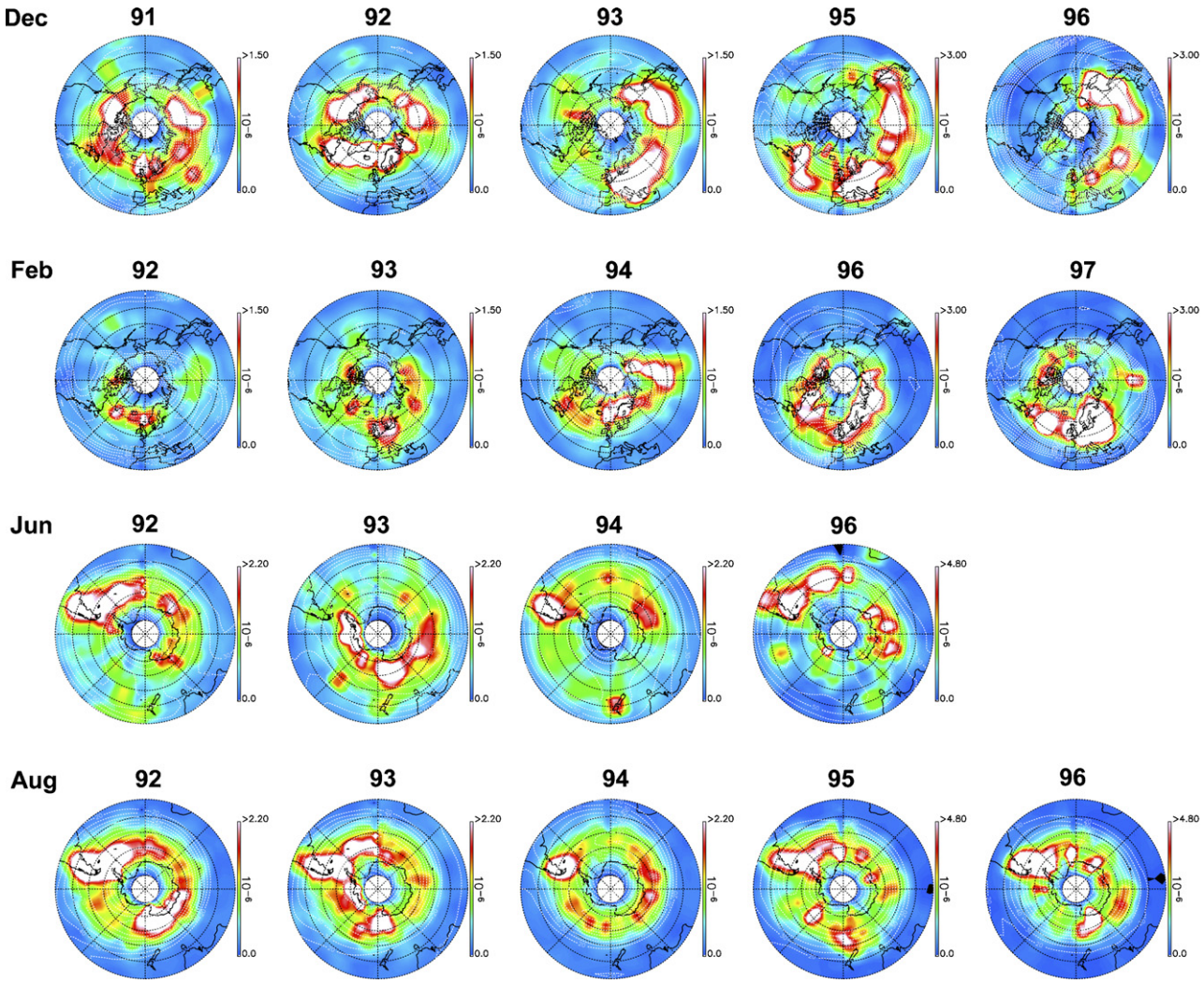

Fig. 4. Multi-year polar maps of 38 km normalized radiance variances during 15–31 December (first-row); 15–28 February (second-row); 15–30 June (third-row); and 15–31 August (forth-row). Data for northern latitudes are measured from UARS MLS north-looking orbits; data from southern orbits are measured from south-looking orbits. The maps for 1992, 1993, and 1994 (left three columns) are averaged over the half-month period as stated above. The maps for 1995, 1996, and 1997 are averaged over available observation days, which are fewer in number than the half-month period.

et al., 2002; Wu and Jiang, 2002). Wave variance changes from year to year, sometimes following the inter-annual changes in peak vortex winds. For example, in late February 1993 and late February 1996, when the Arctic vortex was shifted far off the pole and tilted toward the Atlantic, gravity wave activity centers were mostly moved toward southern Greenland and eastern Europe. In contrast, in late February 1994, when the Arctic vortex was more pole-centered, most wave activities were seen over the northern and eastern Europe.

3. Concluding remarks

We have presented and discussed both the mean climatology and inter-annual variations of gravity wave activity in the polar middle atmosphere as gleaned from along-track fluctuations in ~6 years of limb radiances acquired by the UARS MLS. The results we presented here present a baseline climatology and reference data sets for gravity wave studies with next generation satellite instruments. For example, radiances from the Advanced Microwave Sounding Unit (AMSU) on board the recently launched NASA Aqua satellite have provided similar wintertime hemispheric maps of inferred gravity wave activity (see Fig. 5) (Wu, 2004). The time evolution and spatial distribution of high-latitude gravity waves and their effect on stratospheric circulation, temperature and PSC formation are critical for global modeling assessments of Arctic and Antarctic ozone loss during winter and climate trends (Austin et al., 2003). The existing UARS MLS global gravity wave measurements and the upcoming Aura MLS observations, as well data from other high-resolution satellite instruments (e.g., AMSU, AIRS), offer researchers an unprecedented opportunity for acquiring a long-term global gravity wave data base for atmospheric science studies.

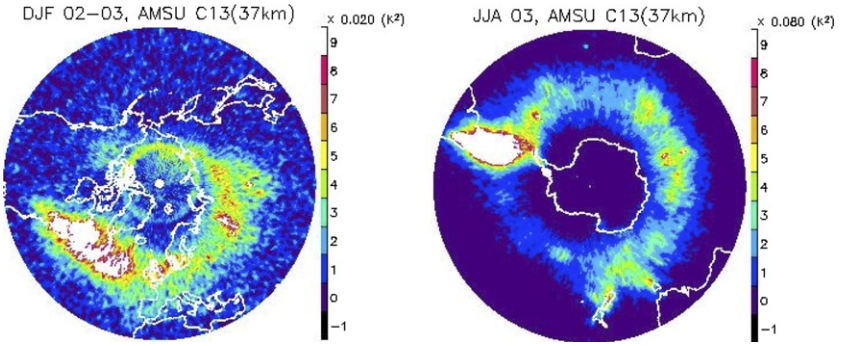

Fig. 5. Seasonal gravity wave variance maps derived from AMSU-A measurements for December–February 2002–2003 (left) and June–August 2003 (right). The altitude is ~37 km. See Wu (2004) for details on the instrument and analysis method.

Acknowledgments

This study was supported by the Jet Propulsion Laboratory, California Institute of Technology, under contract with NASA. The authors also acknowledge the support of the Office of Naval Research through the Naval Research Laboratory's 6.1 research program, NASA Office of Space Science's Geospace Sciences Program, and the Forschungszentrum Karlsruhe GmbH und Universität Karlsruhe, Institut für Meteorologie und Klimaforschung (IMK), Karlsruhe, Germany. Jonathan Jiang thanks Prof. Herbert Fischer, Dr. Gabriele Stiller and the IMK science team for helpful comments and suggestions on this manuscript.

References

Alexander, M.J. Interpretations of observed climatological patterns in stratospheric gravity wave variance. J. Geophys. Res. 103, 8627–8640, 1998.

Austin, J., Shindell, D., Beagley, S.R., Brühl, C., Dameris, M., Manzini, E., Nagashima, T., Newman, P., Pawson, S., Pitari, G., Rozanov, E., Schnadt, C., Shepherd, T.G. Uncertainties and assessments of chemistry-climate models of the stratosphere. Atmos. Chem. Phys. 3, 1–27, 2003.

Carslaw, K.S., Peter, T., Bacmeister, J.T., Eckermann, S.D. Widespread solid particle formation by mountain waves in the Arctic stratosphere. J. Geophys. Res. 104, 1827–1836, 1999.

Dhaniyala, S., McKinney, K.A., Wennberg, P.O. Lee-wave clouds and denitrification of the polar stratosphere. Geophys. Res. Lett. 29 (9), 1422, doi:10.1029/2001GL013900, 2002.

Dörnbrack, A., Birner, T., Fix, A., Fientje, H., Meister, A., Schmid, H., Browell, E.V., Mahoney, M.J. Evidence for inertia gravity waves forming polar stratospheric clouds over Scandinavia. J. Geophys. Res. 107 (20), 8287, doi:10.1029/2001JD000452, 2002.

Duck, T.J., Whiteway, J.A., Carswell, A.I. Lidar observations of gravity wave activity and Arctic stratospheric vortex core warming. Geophys. Res. Lett. 25, 2813–2816, 1998.

Duck, T.J., Whiteway, J.A., Carswell, A.I. The gravity wave-Arctic stratospheric vortex interaction. J. Atmos. Sci. 58, 3581–3596, 2001.

Eckermann, S.D., Hirota, I., Hocking, W.K. Gravity-wave and equatorial-wave morphology of the stratosphere derived from long-term rocket soundings. Quart. J. Roy. Meteor. Soc. 121, 149–186, 1995.

Fueglistaler, S., Luo, B.P., Voigt, C., Carslaw, K.S., Peter, T. NAT-rock formation by mother clouds: a microphysical model study. Atmos. Chem. Phys. 2, 93–98, 2002.

Jiang, J.H., Wu, D.L., Eckermann, S.D. Upper Atmosphere Research Satellite (UARS) MLS observation of mountain waves over the Andes. J. Geophys. Res. 107, D20, doi:10.1029/2002JD002091, 2002.

Jiang, J.H., Wu, D.L., Eckermann, S.D., Ma, J. Mountain waves in the middle atmosphere: Microwave limb sounder observations and analyses. Adv. Space Res. 32, 801–806, 2003.

Jiang, J.H, Eckermann, S.D., Wu, D.L., Ma, J. A search for mountain waves in MLS stratospheric limb radiances from the winter northern hemisphere: data analysis and global mountain wave modeling. J. Geophys. Res. 109 (D3), D03107, doi:10.1029/2003JD003974, 2004a.

Jiang, J.H, Wang, B., Goya, K., Hocke, K., Eckerman, S.D., Ma, J., Wu, D.L., Read, W.G. Geographical distribution and inter-seasonal variability of tropical deep convection: UARS MLS observations and analyses. J. Geophys. Res. 109 (D3), D03111, doi:10.1029/2003JD003756, 2004b.

Jiang, J.H., Wang, D.Y. Methods for calculating gravity wave energy and momentum flux from satellite observations, (in preparation).

Manson, A.H., Meek, C.E., Zhan, Q. Gravity wave spectra and direction statistics for the mesosphere as observed by MF radars in the Canadian Prairies (49–52°N) and Tromsø (69°N). J. Atmos. Terr. Phys. 59, 993–1009, 1997.

McLandress, C., Alexander, M.J., Wu, D.L. Microwave limb sounder observations of gravity waves in the stratosphere: a climatology and interpretation. J. Geophys. Res. 105, 11947–11967, 2000.

Vincent, R.A., Fritts, D.C. A climatology of gravity wave motions in the mesopause region at Adelaide, Australia. J. Atmos. Sci. 44, 748–760, 1987.

Waugh, D.W., Rong, P.P. Interannual variability in the decay of lower stratospheric Arctic vortices. J. Meteorol. Soc. Japan 80, 997–1012, 2002.

Wu, D.L. Horizontal wavenumber spectrum of MLS radiances. J. Atmos. Solar-Terr. Phys. 63, 1465–1477, 2001.

Wu, D.L. Mesoscale gravity wave variances from AMSU – a radiances. Geophys. Res. Lett. 28 (12), doi:10.1029/2004GL019562, 2004.

Wu, D.L., Jiang, J.H. MLS observations of atmospheric gravity waves over Antarctica. J. Geophys. Res. 107 (D24), 4773, doi:10.1029/2002JD002390, 2002.

Wu, D.L., Waters, J.W. Gravity-wave-scale temperature fluctuations seen by the UARS MLS. Geophys. Res. Lett. 23, 3289–3292, 1996.

Wu, D.L., Waters, J.W. Observations of gravity waves with the UARS Microwave Limb Sounder, in: Gravity Wave Processes, NATO ASI Series I: Global Environment Change, vol. 50, pp. 103–120, 1997.